Journal of Applied Electrochemistry (2021) 51:283–293
https://doi.org/10.1007/s10800-020-01502-4

RESEARCH ARTICLE

Designing of a stable and selective glucose biosensor by glucose oxidase immobilization on glassy carbon electrode sensitive to H_2O_2 via nanofiber interface

Zülfikar Temoçin[1]

Received: 15 June 2020 / Accepted: 27 October 2020 / Published online: 15 November 2020

Abstract
The integration of the enzymes on the solid electrode surfaces is an indispensable step for the construction of the bioelectrochemical electrode. In the current work, the blend nanofibers consisting of poly (vinyl alcohol) and poly(ethyleneimine) were deposited by the electrospinning method on an H_2O_2-sensitive modified glassy carbon electrode. Glucose oxidase was immobilized on the glutaraldehyde-activated blend nanofibers. Bioelectrochemical electrode displayed a good linear response to the glucose concentration ranges with two separate calibration curves, from 2 to 8 mmol L^{-1} and from 10 to 30 mmol L^{-1}. Besides, it showed a high anti-interference performance against ascorbic and uric acids as well as long-term storage stability over 63 days. Moreover, analysis results in a diluted human serum sample showed that the prepared bioelectrochemical electrode has the ability to measure glucose in real samples.

Graphic abstract

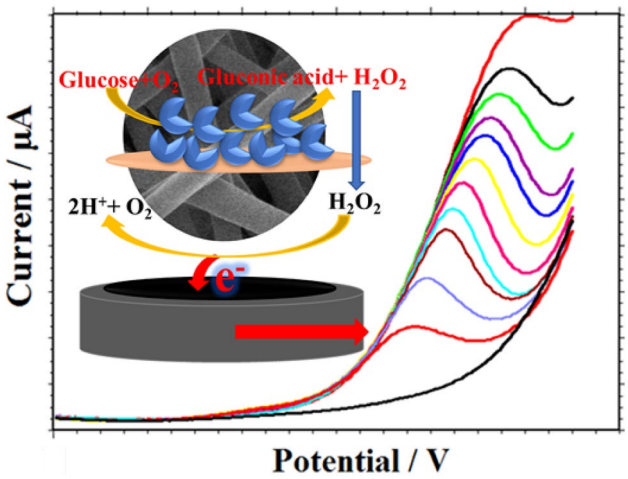

Keywords Glassy carbon · Glucose oxidase · Nanofiber · Glucose biosensor · Poly(vinyl alcohol)

1 Introduction

In recent years, much research has been conducted over bioelectrochemical electrodes (BEC), which are employed for the recognition of various target analytes [1–3]. These constructed electrodes often employ one or more enzymes to exploit the functions tendered by natural structures of

Electronic supplementary material The online version of this article (https://doi.org/10.1007/s10800-020-01502-4) contains supplementary material, which is available to authorized users.

✉ Zülfikar Temoçin
ztemocin@kku.edu.tr

[1] Department of Chemistry, Faculty of Arts and Sciences, Kırıkkale University, Yahşihan, 71450 Kırıkkale, Turkey

enzymes. Especially, reduction–oxidation enzymes have been considerably used in biosensor development due to their ability to catalyze reactions based on electron transfer [4–6]. There are two major challenges to the construction of the BECs: (i) assembly of the enzyme onto an electrode surface [7, 8] and (ii) communication between the immobilized enzyme and the electrode [9–11].

Simple immobilization techniques are used to assemble an enzyme on the electrode surface and to provide the necessary microenvironments for the protection of the sensitive structure of the enzymes [7, 12, 13]. Enzymes have been assembled on the electrode by different immobilization techniques such as physical attachment [14, 15], entrapment [16], layer-by-layer assembly [17, 18], and covalent attachment [19]. Among these techniques, the advantage of covalent immobilization is minimized leakage of the immobilized enzyme from the electrode surface, which leads to an increase in the stability of the BEC [20, 21].

Nanofibers are used as support materials because they have a high surface area to volume ratio. They also provide good chemical stability, and alterable porosity, facilitating the development of various sensing devices [22–24]. Enzymes are immobilized on nanofibers by using different immobilization techniques so that nanofibers can provide an interface between electrode and enzymes for the construction of the stable BEC [25–27].

Poly (vinyl alcohol) (PVA) is a biocompatible polymer that has been widely used for enzyme immobilization. Unlike many other polymers, PVA can be electrospun using water as a solvent to form nanofibers. These nanofibers are capable of providing mechanical support for enzyme immobilization [28, 29]. As a water-soluble polymer, poly (ethyleneimine) (PEI) has abundant primary amino groups that able to react with the glutaraldehyde molecule. It is possible to produce PVA-based nanofiber containing PEI by mixing PVA and PEI solutions by electrospinning technique [30, 31]. In this way, blend nanofiber bearing amine groups is obtained. Several support materials containing amine groups have been widely used for covalent immobilization of enzymes [32, 33].

Communication between the enzyme and electrode is a very important criterion for generating a measurable current [33–35]. This communication is possible in three different ways: (i) product-based communication resulting from the catalytic activity of enzymes. The products of this catalytic activity are exposed to electrochemical oxidation or reduction, which takes place on the electrode, generating a measurable current [36–38], (ii) mediator-based communication [16, 39], and (iii) the direct electron transfer-based communication [34, 40]. Modification of the solid electrode surface is an important part of the electrochemical biosensor studies for obtaining a sensitive and selective BEC [41, 42].

The aim of this study was to design a stable and selective glucose biosensor with a measuring range that can be used for direct glucose measurement in blood samples of healthy people and diabetic patients requiring neither stirring nor dilution of the samples. In this work, an H_2O_2-sensitive modified glassy carbon electrode (MGC) was prepared by the electrochemical treatment method [43]. Glucose oxidase (GOx) was chosen as a model enzyme to construct BEC on MGC. The reason why GOx was used is that the catalytic activity of GOx generates H_2O_2 and also it has a low cost [44–46]. The PEI/PVA blend nanofibers were used as a biocompatible platform for enzyme immobilization in the development of enzyme-based biosensor. PEI/PVA blend nanofibers were employed on the electrode surface as fixation material to obtain stabilized GOx molecules. To fabricate BEC, the surface of MGC was coated with PEI/PVA blend nanofibers via electrospinning technique. After the activation of the amine groups of PEI with glutaraldehyde, the GOx was immobilized on the blend nanofiber [47]. The whole fabrication strategy of the BEC is shown in Scheme 1. The prepared BEC performs glucose detection depending on two basic reactions. The first is that GOx, immobilized on

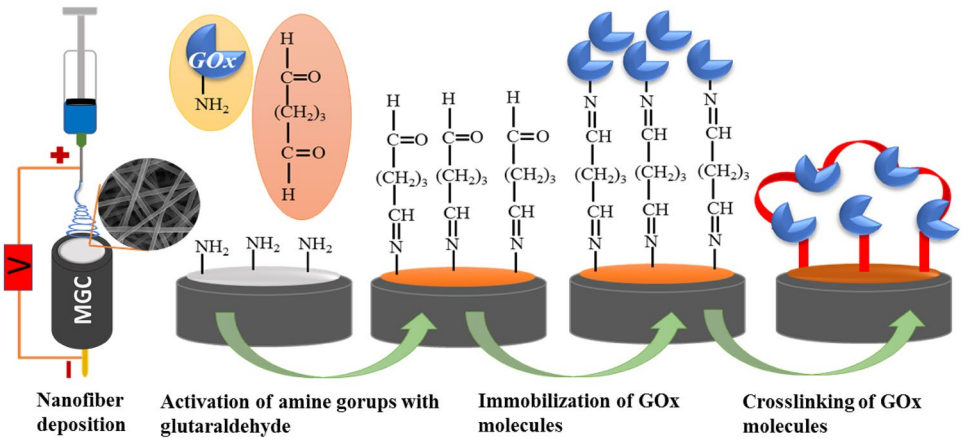

Scheme 1 Schematic description of the GOx-based BEC construction

the PEI/PVA blend nanofibers, converts the glucose into gluconic acid. In the meantime, a second product of the enzymatic reaction, electroactive H_2O_2 is also formed [44]. The PEI/PVA blend nanofibers on the surface of the MGC are permeable to diffusible species and are nonconducting. The H_2O_2 formed as a result of the oxidation of glucose moves along this permeable nanofiber structure and reaches the MGC surface. The electrocatalytic decomposition of H_2O_2 under oxidative electrode voltage causes electron transfer from H_2O_2 to the MGC. This electrocatalytic decomposition results in the generation of a measurable electrical signal that represents the glucose concentration. The constructed BEC was used for specific glucose measurements in the solution under non-stirred conditions. It was also tested for reusability, storage stability, and anti-interference ability. Finally, the BEC was used for glucose analysis in a diluted human blood serum sample.

The most important result of this study is that the prepared BEC exhibited a suitable linear range for glucose detection without dilution from blood samples of healthy and diabetic patients under non-stirred media. The prepared BEC also demonstrated high performance in reuse and storage stability as well as in selectivity.

2 Materials and methods

2.1 Materials

Glucose oxidase (from *Aspergillus niger*, type X-S), PEI aqueous solution (50 wt%), and fructose were purchased from Sigma. PVA (M_w is 145.000 g mol^{-1}), glutaraldehyde (25 wt%), sodium hydroxide, sodium dihydrogen phosphate, glucose, mannose, galactose, and sucrose were purchased from Merck. All aqueous solutions were prepared with deionized water from an Elga Purelab Classic water purification system.

2.2 Instruments

Phywe HV-power supply (Germany) was used to produce a high voltage for the preparation of the nanofiber. The polymer solution feed rate was controlled by a syringe pump (New Era, USA). Bruker Vertex 70 V FT-IR spectrophotometer (Bruker, Ettlingen, Germany) was used to obtain infrared spectra. Scanning electron microscope (SEM) photograph was taken by Zeiss EVO LS10 (Germany) for the observation of the form and diameter of the nanofibers (working voltage: 25 kV). UV–Visible (UV–Vis) absorption spectra of the GOx solution, and the films were recorded with a Perkin Elmer Lambda 35 (USA) spectrophotometer. Electrochemical experiments were performed on a CHI 660B electrochemical workstation (CH instrument, USA). Electrochemical experiments were carried out at room temperature (23 ± 2 °C) with a glassy carbon electrode (GC) (3.0 mm diameter, CHI) as the working electrode, a commercial Ag/AgCl (3 M KCl) electrode (CHI) as the reference, and a Pt wire as the counter electrode.

2.3 Preparation of H_2O_2-sensitive MGC

The GC was cleaned with 0.3 and then 0.05 µm alumina slurry and finally washed in an ultrasonic deionized water bath for 3 min. The MGC was prepared by the cyclic voltammetry technique in a 0.5 mol L^{-1} sodium hydroxide solution. The electrical potential was changed from 0.0 to 1.0 V with a scan rate of 30 mV s^{-1}. The MGC was rinsed with deionized water and then stored in a phosphate buffer (PB) solution (50 mmol L^{-1}, pH 7.1).

2.4 Preparation of the nanofiber-coated MGC

The PVA solution (0.12 g mL^{-1}) was prepared by dissolving the PVA granules in boiling deionized water. After cooling the PVA solution to 25 °C, the PVA solution was mixed with adequate amount of PEI solution (50% w/w) and deionized water under magnetic stirring for 2 h to achieve a homogeneous solution (final concentrations of PVA and PEI are 0.1 g mL^{-1} and 0.02 g mL^{-1}, respectively). The PEI/PVA solution was loaded into a plastic syringe equipped with a stainless-steel needle. The PEI/PVA blend nanofibers were deposited on the MGC by electrospinning technique. The nanofibers were deposited by applying a high voltage of 20 kV to the needle tip and MGC with 8 cm spacing between them. The mixed polymer solution was fed at a rate of 10 µL min^{-1} using a syringe pump. The nanofibers on MGC were dried for 2 h at room temperature.

2.5 Enzyme loading on PEI/PVA nanofiber-coated MGC

The nanofiber-coated MGC was incubated for 5 h in glutaraldehyde solution (1%w/w) for activation of amine groups of PEI in nanofibers structure [48]. Following the activation step, the electrode was washed in deionized water to remove the unattached glutaraldehyde. A 20 µL of the GOx solution (10 mg mL^{-1}, pH 7.1) was dropped onto the glutaraldehyde-activated PEI/PVA nanofiber-coated MGC and kept at room temperature for 1 h for covalent binding of the enzyme. Then a 10 µL of the glutaraldehyde solution (0.1%w/w) was dropped onto the enzyme-immobilized electrode surface for crosslinking of GOx molecules and kept at room temperature for 1 h [49, 50]. Then the electrode was washed in deionized water to remove the loosely bound molecules. The prepared BEC was stored at + 4 °C in PB solution (pH 7.1).

2.6 UV–Visible spectroscopic measurements

For UV–Visible absorption measurement, the PEI/PVA film (about 1 mm thickness) was prepared by drying the PEI/PVA solution (PVA and PEI were 0.1 g mL^{-1} and 0.02 g mL^{-1}, respectively) in a petri dish for 48 h at 40 °C. Then the PEI/PVA film was cut into test sections in appropriate sizes (about 1 × 2 cm). The GOx was immobilized on the PEI/PVA blend structure after the activation of the film with glutaraldehyde. The PEI/PVA film was rinsed three times in the PB solution after each step. The film was dried at room temperature before UV–visible absorption measurement.

2.7 Electrochemical measurements

Differential pulse voltammetry (DPV) parameters were adjusted to a scan rate of 0.025 V s^{-1}, 0.05 V pulse amplitude, and 0.05 s pulse width. Electrochemical measurements were carried out in a 1 mL solution under non-stirred conditions. The electrochemical measurements were performed immediately after the electrode was immersed in the solution. The current value was calculated as the average of three different measurements.

3 Results and discussion

3.1 H_2O_2 sensitivity of the MGC

In order to improve the H_2O_2 sensitivity of the GC, the GC was modified by electrochemical treatment method in a basic solution. The electrochemical modification of the GC was performed under the potentiodynamic conditions where the potentials were cycled between 0.0 V and + 1.0 V for 20 cycles (Fig. S1 in the Supporting Information shows the cyclic voltammograms for this experiment). The current increases were measured during the 1st and 20th potential cycles of the electrochemical treatment. These changes in current values demonstrate that the surface properties of the GC were improved for electrocatalytic oxidation of some biomolecules [43]. The electrocatalytic properties of the GC and MGC were investigated using the DPV technique in the 5 mmol L^{-1} H_2O_2 solutions (pH 7.1). As shown in Fig. 1A, a relatively broad and weak peak was observed at about + 1.20 V at the GC. However, the MGC, changing the peak potential to + 0.92 V, produced more clear peak shape and pretty high peak current. The changing peak potential and increasing peak current indicate that the MGC has an electrocatalytic effect on the H_2O_2 oxidation. Figure 1B illustrates the response of MGC on different H_2O_2 concentrations. The DPV voltammograms clearly show that the oxidation peak currents were gradually increased with the increase in concentrations of the H_2O_2. These results suggest that the MGC has the ability of product-based electrochemical communication with H_2O_2 produced by the catalytic activities of the enzymes.

3.2 Characterization of the nanofibers and immobilized enzyme

PEI/PVA nanofibers were used as an immobilization platform for GOx. To this end, the MGC was coated with PEI/PVA nanofibers. The surface morphology of PEI/PVA nanofibers was characterized by SEM. Figure 2A shows the formation of uniform PEI/PVA nanofibers stacked randomly on each other with a web appearance. The diameters of nanofibers are ranged from 350 to 500 nm. As revealed by the SEM image, the nanofiber structure of PEI/PVA was formed on the MGC.

After activation of the nanofibers with glutaraldehyde, the GOx was immobilized on nanofibers. The immobilized GOx molecules were crosslinked with glutaraldehyde to prevent the enzyme leakage from the surface and to improve the enzyme stability. To verify the successful preparation of the GOx-immobilized nanofiber, FT-IR spectra of the PVA nanofibers, PEI/PVA nanofibers, glutaraldehyde-activated PEI/PVA nanofibers, and GOx-immobilized nanofibers were obtained for structural characterization (Fig. 2B). As shown in (a) section of Figure that represents the FT-IR spectrum of PVA nanofibers, the broadband at 3300 cm^{-1} indicates

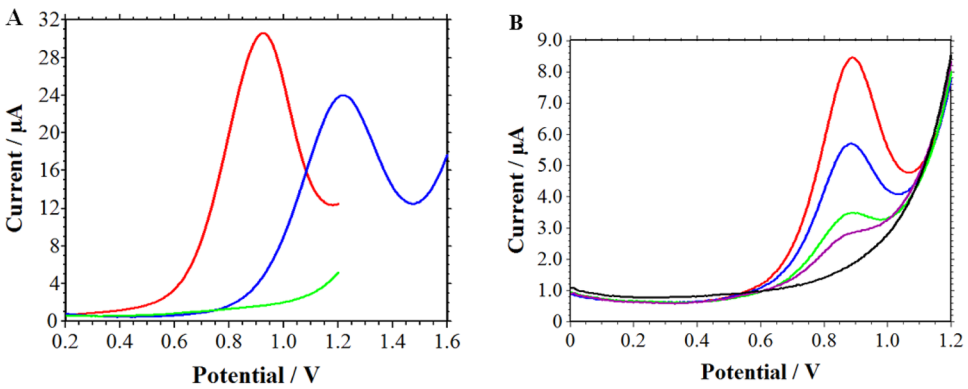

Fig. 1 **A** DPV voltammograms of GC (——), MGC (——) in the presence of 5 mmol L^{-1} H_2O_2 and MGC (——) in only PB (PB solution: 50 mmol L^{-1}, pH 7.1). **B** DPV voltammograms of MGC in PB solutions (50 mmol L^{-1}, pH: 7.1) containing various concentrations of H_2O_2 (—— 1, —— 0.5, —— 0.2, —— 0.1 mmol L^{-1}, —— only PB). (Color figure online)

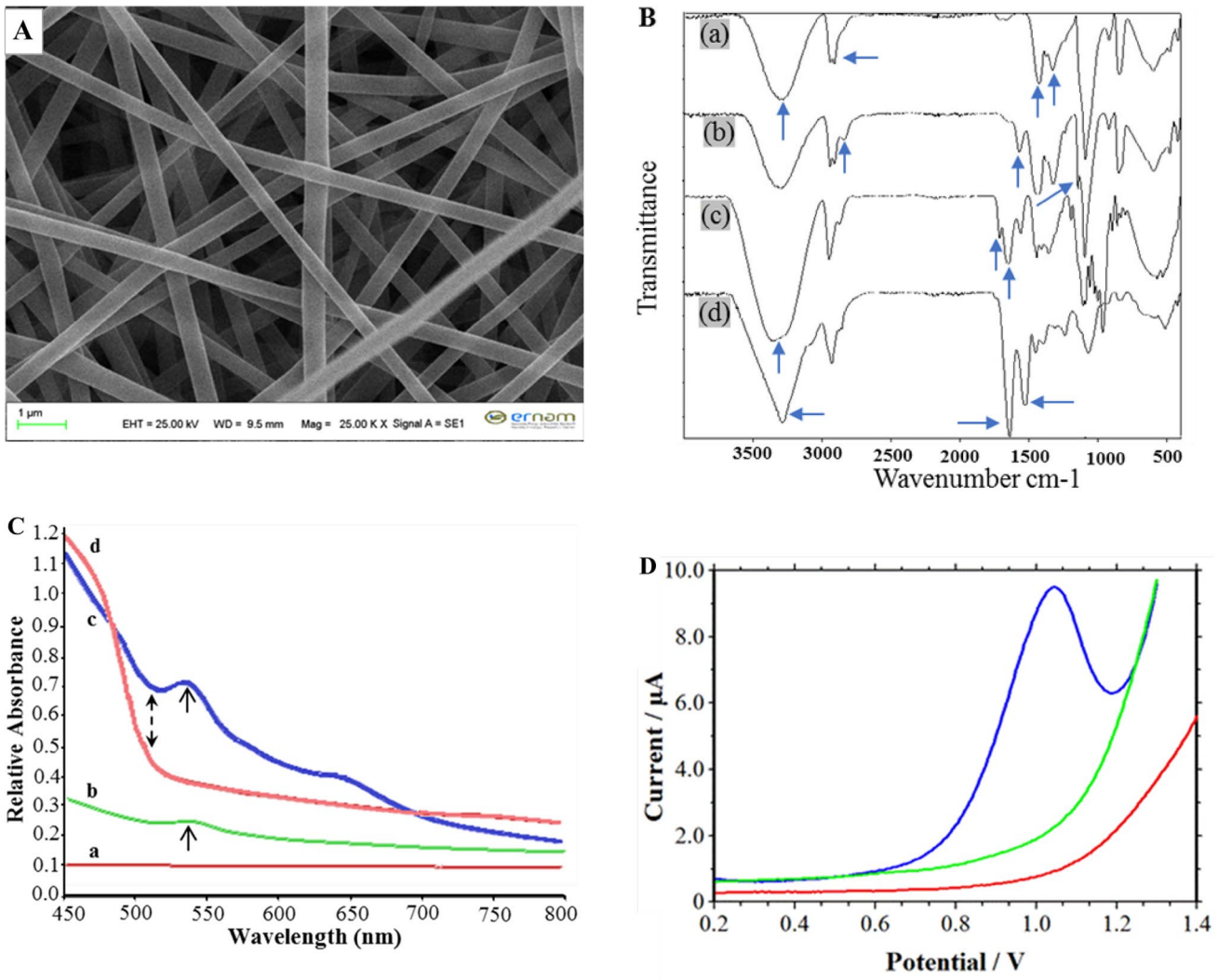

Fig. 2 **A** SEM image of PEI/PVA blend nanofiber. **B** FT-IR spectra of nanofibers. PVA nanofibers (a), PEI/PVA nanofibers (b), glutaraldehyde-activated nanofibers (c), and GOx-immobilized nanofibers (d). **C** UV–visible absorption spectra. PEI/PVA film (a), glutaraldehyde-activated PEI/PVA film (b), GOx-immobilized PEI/PVA film (c), and GOx solution (d). **D** DPV voltammograms in PB solutions. GC (—), BEC (—) in the presence of 5 mmol L^{-1} glucose, and BEC (—) in only PB (PB solution: 50 mmol L^{-1}, pH 7.1). (Color figure online)

the OH stretching peak. The peak at about 2900 cm^{-1} is stretching vibrations (CH). The peaks at 1420 cm^{-1} and 1320 cm^{-1} can be attributed to bending vibrations (OH and CH). In (b) section of Figure, the new peaks at 2840 cm^{-1}, 1580 cm^{-1}, and 1140 cm^{-1} correspond to stretching and bending vibration peaks of amine groups of PEI. These results confirm that PEI is involved in the PVA nanofiber structure. As shown in (c) section of Figure, the broad peak at 3350 cm^{-1} can be related to the aldehyde groups of the glutaraldehyde on nanofibers. The peak at 1712 cm^{-1} (C=O) was ascribed to carbonyl groups (free) of the glutaraldehyde, and the peak at 1640 cm^{-1} (C=N) was attributed to the imine bond formed by reaction between aldehyde and amine of PEI. These findings show that glutaraldehyde is bound to the nanofibers, and this nanofiber structure contains the free aldehyde groups for enzyme immobilization. The spectrum in the (d) section of Fig. 2B shows some remarkable changes resulting from the reaction of the glutaraldehyde with the amino group of GOx. The peak shape at 3300 cm^{-1} changed and the intensity of peaks at 1630 cm^{-1} and 1530 cm^{-1} increased. These changes can be attributed to the formation of the new imine groups by the reaction of the aldehyde groups with the amine groups of the enzyme. Furthermore, the peptide bonds of the GOx give rise to several amide vibrations. The findings confirm the immobilization of GOx molecules on PEI/PVA nanofibers.

The UV–Visible spectroscopic measurements could provide information about confirmation for the GOx

immobilization on the PEI/PVA blend structure. Figure 2C shows the spectra of the PEI/PVA film, the glutaraldehyde-activated PEI/PVA film, and the GOx-immobilized PEI/PVA film. The spectrum of the GOx solution was also taken for comparison. As shown from the figure, the PEI/PVA film (curve a) did not show any absorption peak in the examined spectral region. However, the glutaraldehyde-activated PEI/PVA film (curve b) showed a weak absorption peak around 538 nm. This peak can be attributed to the imine bond formed by the reaction between aldehyde and amine of PEI. The spectrum of the GOx-immobilized PEI/PVA film (curve c) showed a more intense peak at the same wavelength. This increase in peak intensity can be attributed to more imine bonds formed by the crosslinking of the GOx with glutaraldehyde on the film surface. This difference shows that the GOx was immobilized on the PEI/PVA blend structure. The examination of the spectrum of the GOx solution (curve d) revealed an increase in the absorbance values of the spectrum between 510 and 450 nm wavelength. The spectrum of the GOx-immobilized PEI/PVA film showed a similar increase to the spectrum of the GOx solution in the same region. (The starting points of the increase are marked on the figure with a double arrow.) The results indicated that the GOx was immobilized on the PEI/PVA blend structure.

To provide more definitive evidence for the immobilization of GOx on the MGC, the responses of the GC and the BEC to the glucose solution (5 mmol L^{-1}) were compared using the DPV technique. The DPV voltammograms of the GC and the BEC were given in Fig. 2D. As seen in the figure, no response of the GC to glucose was obtained. In contrast, the BEC showed a defining peak dependent on glucose, which indicates that the GOx was immobilized on the MGC surface by nanofibers and continues its activity.

Besides, the cyclic voltammetry technique was used to produce new evidence for the GOx immobilization. To this end, the cyclic voltammograms of GC, PVA nanofiber-coated MGC, PEI/PVA nanofiber-coated MGC, glutaraldehyde-activated PEI/PVA nanofiber-coated MGC, and the GOx immobilized on MGC by nanofibers were taken in glucose solution (Fig. S2 in the Supporting Information shows the cyclic voltammograms for this experiment). The voltammogram of the GOx-immobilized MGC was the only one that showed the peak defining the glucose molecule (at about + 1.0 V). The other four voltammograms exhibited a similar shape. No peak representing glucose occurred on these voltammograms, thus indicating that the GOx was immobilized on the MGC surface by nanofibers and showed its activity for glucose detection.

3.3 The response of the BEC to glucose solutions

The analysis performing skill of the prepared BEC was measured with various glucose concentrations (pH 7.1)

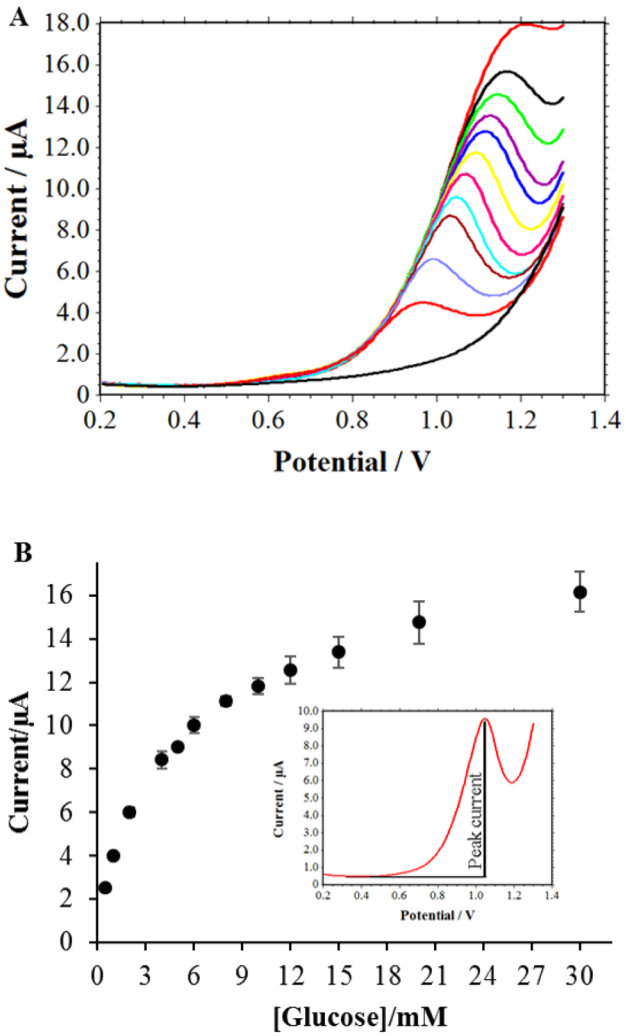

Fig. 3 **A** DPV voltammograms of BEC in PB solutions (50 mmol L^{-1}, pH: 7.1) with different glucose concentrations (30, 20, 15, 12, 10, 8, 6, 5, 4, 2, 1 mmol L^{-1}, only PB). **B** Peak current values of BEC for different concentrations of glucose. Inset: Method of determining peak current value. (Color figure online)

from 1 to 30 mmol L^{-1}. In Fig. 3A, DPV voltammograms display the response of the BEC to different glucose concentrations. The peak currents of the voltammograms rose as the amount of glucose in solutions was increased. Figure 3B shows the peak current values corresponding to the glucose concentrations. The peak current of DPV voltammograms was calculated using the software of CHI 660 B electrochemical workstation as depicted in the inset of Fig. 3B. As can be seen from the figure, the concentration-dependent current increase rate did not show the same tendency throughout the studied glucose concentration values. This can be attributed to the limited number of enzymes immobilized on the electrode surface [51, 52]. The peak current

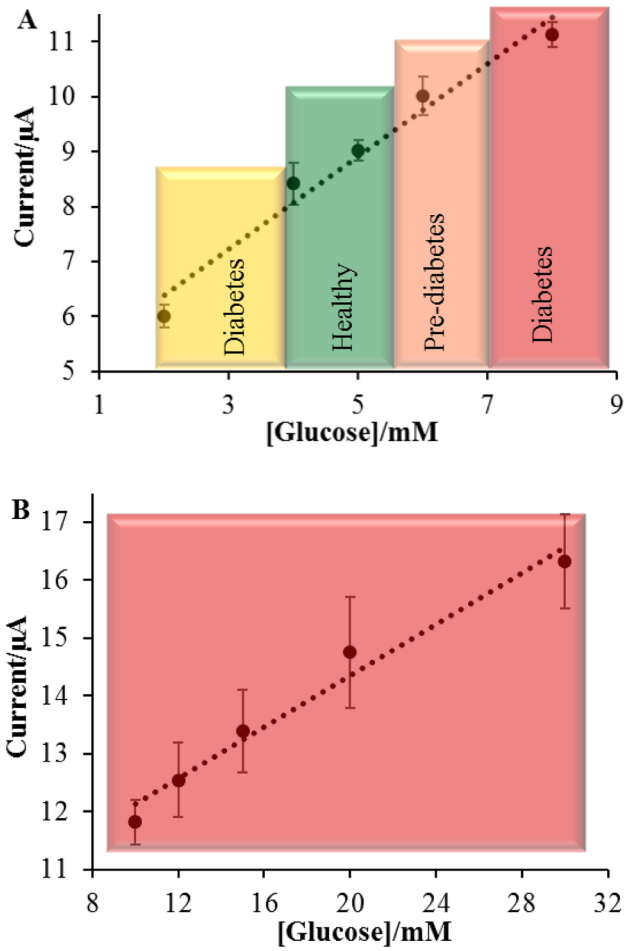

Fig. 4 **A** Calibration curve of the peak current vs. the concentration of glucose: Ip vs [Glucose] = 2, 4, 5, 6, 8 mmol L^{-1}, equation: I (μA) = 4.686 ± 0.459 + 0.846$C_{glucose}$ ± 0.085(mmol L^{-1}) (R^2 = 0.971), **B** Calibration curve of the peak current vs. the concentration of glucose: Ip vs [Glucose] = 10, 12, 15, 20, 30 mmol L^{-1}, equation: I (μA) = 9.912 ± 0.399 + 0.222$C_{glucose}$ ± 0.021(mmol L^{-1}) (R^2 = 0.973)

values and glucose concentrations can exhibit significantly good linear relationships in two sections. Figure 4A and B shows the calibration curves of these sections. The first section spans from 1 to 8 mmol L^{-1} of glucose concentrations. The second section includes the glucose concentration range from 10 to 30 mmol L^{-1}. The sensitivities were 11.79 μA mmol L^{-1} cm^{-2} for the first linear range and 3.19 μA mmol L^{-1} cm^{-2} for the second linear range with a detection limit of 0.3 mmol L^{-1}. These calibration curves of the BEC are good enough to compute glucose concentrations of both healthy and diabetic patients [53].

3.4 Interference study

Coexisting with glucose in real samples, such electrochemical interfering agents as ascorbic acid, uric acid, and sugar forms cause one major problem in glucose analysis. The interference effect causes an increase or decrease in the signal generated by the target molecule, which affects the accuracy of the biosensor [54–56]. Thus, the anti-interference performance of the constructed BEC was also tested towards some biomolecules such as ascorbic acid, uric acid, fructose, galactose, mannose, and sucrose (Figs. S3, S4, S5, S6, S7, and S8 in the Supporting Information show the DPV voltammograms for the anti-interference performance of the BEC, respectively). In the presence of interfering substances, there is no significant change in the peak current and peak appearance of the glucose, which indicates the good and excellent selectivity of the built BEC. Although the BEC has a high working potential for oxidation of the hydrogen peroxide, the interference effects of the electroactive ascorbic and uric acid molecules were eliminated. The most important reason for this is that the MGC can oxidize ascorbic acid and uric acid molecules at low working potentials (− 0.05 V for ascorbic acid and + 0.25 V for uric acid) [43]. In addition, the high specificity of the GOx to glucose has eliminated the interference effect of sugars [57].

3.5 Stability of the BEC

One important parameter in the assessment of the efficiency of the electrochemical biosensor is stability [58, 59]. The stability of the BEC was determined by three different approaches. First, the operational stability of the BEC was examined in 5 mmol L^{-1} glucose solution. To this end, ten consecutive measurements were performed, each time using a fresh glucose solution. The DPV voltammograms of operational stability are given in Fig. 5A. As can be seen from the figure, there is little fluctuation in the peak current values of voltammograms. The concentrations of glucose from voltammograms were calculated as 5.12 ± 0.3 mmol L^{-1}. These voltammograms indicate that the BEC has good operational stability. As the second step for the determination of the stability, the BEC was used for glucose measurements in five consecutive days. The responses of the BEC to the solutions (pH 7.1) containing 2, 5, and 10 mmol L^{-1} of glucose were measured every day (Fig. S9, S10, and S11 in the Supporting Information show the DPV voltammograms for these experiments, respectively). Then BEC was stored in PB solution + 4 °C. The peak current values in Fig. 5B indicated that the BEC showed very good stability for the measurement of various concentrations of glucose for successive five days.

The long-term stability of enzyme-based biosensors is a challenging issue due to the instability of enzymes [60, 61]. Finally, for the stability test, the BEC was stored in PB solution over 63 days at + 4 °C. The glucose responses of the BEC were recorded by the DPV technique at specific time intervals using glucose solutions having the

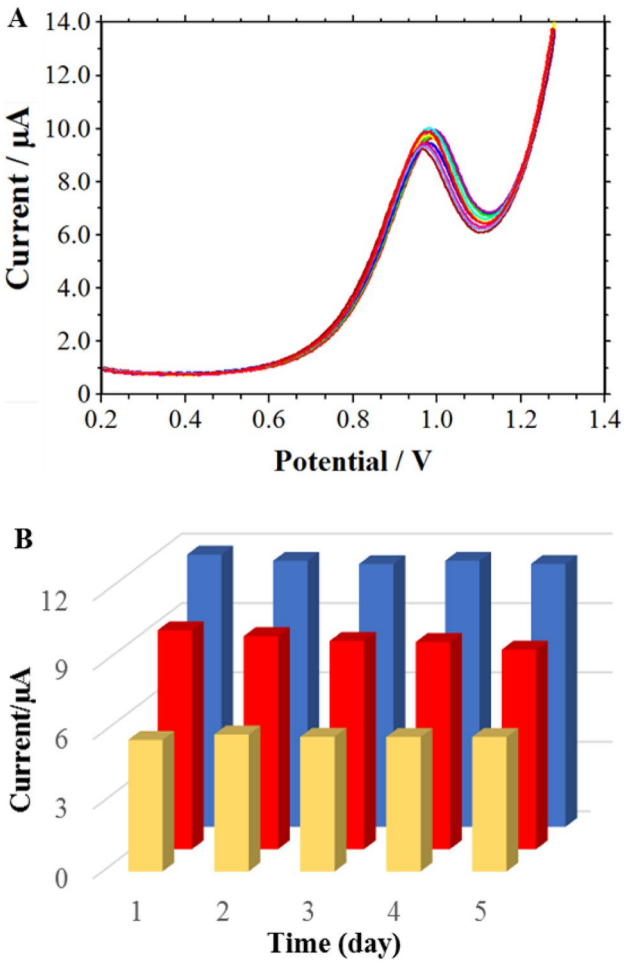

Fig. 5 Stability tests of BEC **A** DPV voltammograms of BEC for ten consecutive glucose (5 mmol L^{-1}) measurements in PB solutions (50 mmol L^{-1}, pH 7.1). **B** The current response of BEC in various concentrations of glucose solutions (2, 5 and 10 mmol L^{-1}) for successive five days. (Color figure online)

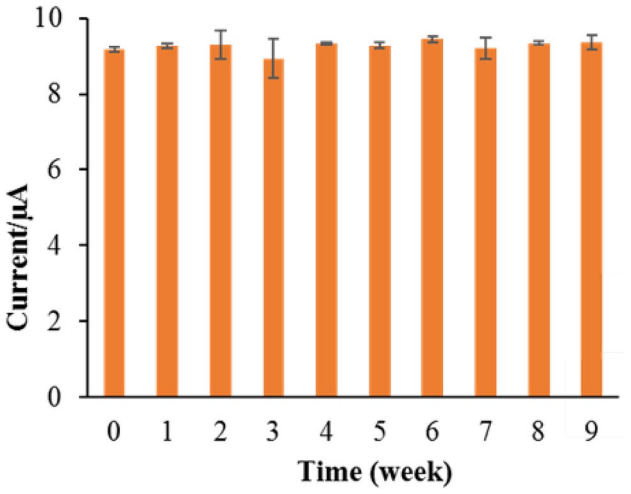

Fig. 6 Storage stability of BEC and the current response of BEC was measured in glucose solution (5 mmol L^{-1}) as a function of storage time

same concentration. (DPV voltammograms are shown in Fig. S12 in the Supporting Information). Figure 6 shows the current values obtained from voltammograms during the storage period. They displayed a maximum decrease of 5.2% and an increase of 3.4% compared to the initial value. These results are indicating that the BEC has excellent long-term stability, which can be ascribed to excellent protection for GOx by the two-step immobilization application. The crosslinking of the GOx provides a robust enzyme-nanofiber network, yielding a compatible microenvironment for preserving the enzyme activity and effectively suppressing enzyme leakage from the nanofiber surface in the storage and glucose analysis conditions [60, 62].

The reproducibility of the analytic signal is among the desired features of biosensors [63, 64]. For this reason, three individual BECs were prepared and used for the detection of glucose in 5 mmol L^{-1} glucose solutions (Figs. S13, S14, and S15 in the Supporting Information show DPV voltammograms of each individual BEC). The relative standard deviation of glucose concentrations calculated by consecutive measurements was found to be 7.5%, indicating that the BECs produced glucose analysis results, which were pretty acceptable in reproducibility. The slight inaccuracy in the results of the analysis might have resulted from the small differences in the level of H_2O_2 sensitivities of the MGCs. Furthermore, the different orientation of the enzyme during immobilization on the electrode surface from the electrode to the electrode can cause different results of glucose analysis.

3.6 Real sample analysis

To demonstrate the usefulness of the prepared BEC in a complex sample, the BEC was used to measure the concentrations of glucose in a human blood serum, which was diluted fifteen times with a PB (50 mmol L^{-1}, pH 7.1) solution (Selected DPV voltammograms are shown in Fig. S16 in the Supporting Information). As shown in Table 1, the results obtained by the BEC are in good agreement

Table 1 Recovery results of the constructed BEC to glucose in a diluted human blood serum sample ($n=3$)

Glucose concentration (mmol L^{-1})		Recovery (%)	RSD (%)
Added	Found		
2	1.92	96.0	6.4
4	4.28	107.0	6.3
6	6.45	107.5	2.8
10	9.59	95.9	8.5

with the amount of glucose added. The recoveries were in the range of 95.9%-107.5%, and the relative standard deviations were less than 9.0%. Experimental results confirmed that the constructed BEC has a practical application for glucose detection in real samples.

4 Conclusions

In this study, a bioelectrochemical electrode was constructed for the assay of glucose in non-stirred samples based on the immobilization of GOx on nanofiber-coated MGC sensitive to H_2O_2. Nanofibers were characterized by SEM film and FT-IR spectra. Covalent immobilization of GOx was also confirmed by FT-IR and UV–Visible spectra. Two-step immobilization method with glutaraldehyde increased the reuse and storage stability of the BEC. The BEC showed a good selective ability for the detection of glucose, and it also eliminated the interference effects of ascorbic and uric acids. In addition, the constructed BEC has an acceptable reproducibility and repeatability of the glucose signal. It has also been tested for the detection of glucose in a human blood serum sample with enough accuracy. To sum up, the BEC constructed for this study showed that nanofiber-coated MGC can be used to fabricate different biosensors based on the use of different enzymes (such as galactose oxidase), the product of which is H_2O_2.

Acknowledgements This work was supported by Scientific Research Projects Coordination Unit of Kırıkkale University (Project Number: 2015-005).

References

1. Tian T, Liu M, Chen L, Zhang F, Yao X, Zhao H, Li X (2020) D-amino acid electrochemical biosensor based on D-amino acid oxidase: mechanism and high performance against enantiomer interference. Biosens Bioelectron 151:111971
2. Bollella P, Hibino Y, Kano K, Gorton L (2018) Highly sensitive membraneless fructose biosensor based on fructose dehydrogenase immobilized onto aryl thiol modified highly porous gold electrode: characterization and application in food samples. Anal Chem 90:12131
3. Akhtar MA, Batool R, Hayat A, Han D, Riaz S, Khan SU, Nasir M, Nawaz MH, Niu L (2019) Functionalized graphene oxide bridging between enzyme and Au-sputtered screen-printed interface for glucose detection. ACS Appl Nano Mater 2:1589–1596
4. Saboe PO, Conte E, Farell M, Bazan GC, Kumar M (2017) Biomimetic and bioinspired approaches for wiring enzymes to electrode interfaces. Energy Environ Sci 10:14–42
5. Huang X, Zhang L, Zhang Z, Guo S, Shang H, Li Y, Liu J (2019) Wearable biofuel cells based on the classification of enzyme for high power outputs and lifetimes. Biosens Bioelectron 124–125:40–52
6. Alam F, Choudhury SR, Jalal AH, Umasankar Y, Forouzanfar S, Akter N, Bhansali S, Pala N (2018) Lactate Biosensing: The emerging point-of-care and personal health monitoring. Biosens Bioelectron 117:818–829
7. Ariga K, Ji Q, Mori T, Naito M, Yamauchi Y, Abe H, Hill JP (2013) Enzyme nanoarchitectonics: organization and device application. Chem Soc Rev 42:6322–6345
8. Castillo GFD, Koenig M, Müller M, Eichhorn KJ, Stamm M, Uhlmann P, Dahlin A (2019) Enzyme immobilization in polyelectrolyte brushes: high loading and enhanced activity compared to monolayers. Langmuir 35:3479–3489
9. Kausaite-Minkstimiene A, Simanaityte R, Ramanaviciene A, Glumbokaite L, Ramanavicius A (2017) Reagent-less amperometric glucose biosensor based on a graphite rod electrode layer-by-layer modified with 1,10-phenanthroline-5,6-dione and glucose oxidase. Talanta 171:204–212
10. Bravo I, Revenga-Parra M, Pariente F, Lorenzo E (2017) Reagentless and robust biosensor for direct determination of lactate in food samples. Sensors 17:144
11. Wu Y, Kong Y, Lu K, Lv M, Ye Y, Zhao Y (2017) An easy fabrication of glucose oxidase-dipeptide-reduced graphene oxide nanocomposite for glucose sensing. Mater Res Bull 94:378–384
12. Kim E, Xiong Y, Cheng Y, Wu HC, Liu Y, Morrow BH, Ben-Yoav H, Ghodssi R, Rubloff GW, Shen J, Bentley WE, Shi X, Payne GF (2015) Chitosan to connect biology to electronics: fabricating the bio-device interface and communicating across this interface. Polymers 7:1–46
13. Shi XW, Qiu L, Nie Z, Xiao L, Payne GF, Du Y (2013) Protein addressing on patterned microchip by coupling chitosan electrodeposition and "electro-click" chemistry. Biofabrication 5:041001
14. Schulz C, Ludwig R, Gorton L (2014) Polyethyleneimine as a promoter layer for the immobilization of cellobiose dehydrogenase from *Myriococcum thermophilum* on graphite electrodes. Anal Chem 86:4256–4263
15. Guo Q, Liu L, Zhang M, Hou H, Song Y, Wang H, Zhong B, Wang L (2017) Hierarchically mesostructured porous TiO_2 hollow nanofibers for high performance glucose biosensing. Biosens Bioelectron 92:654–660
16. Dinesh B, Devi KSS, Krishnan UM (2019) Achieving a stable high surface excess of glucose oxidase on pristine multiwalled carbon nanotubes for glucose quantification. ACS Appl Bio Mater 2:1740–1750
17. Si Y, Park JW, Jung S, Hwang GS, Goh E, Lee HJ (2018) Layer-by-layer electrochemical biosensors configuring xanthine oxidase and carbon nanotubes/graphene complexes for hypoxanthine and uric acid in human serum solutions. Biosens Bioelectron 121:265–271
18. Godman NP, DeLuca JL, McCollum SR, Schmidtke DW, Glatzhofer DT (2016) Electrochemical characterization of layer-by-layer assembled ferrocene-modified linear poly(ethylenimine)/enzyme bioanodes for glucose sensor and biofuel cell applications. Langmuir 32:3541–3551
19. Shervedani RK, Foroushani MS (2016) Comparative electrochemical behavior of proteins; cytochrome c, *Agaricus bisporus* laccase, and glucose oxidase, immobilized onto gold-thiol self-assembled monolayer via electrostatic, covalent, and covalent coordinate bond methods. Electrochim Acta 187:646–654
20. Manoj D, Theyagarajan K, Saravanakumar D, Senthilkumar S, Thenmozhi K (2018) Aldehyde functionalized ionic liquid on electrochemically reduced graphene oxide as a versatile platform for covalent immobilization of biomolecules and biosensing. Biosens Bioelectron 103:104–112
21. Feizabadi M, Soleymanpour A, Faridnouri H, Ajloo D (2019) Improving stability of biosensor based on covalent immobilization of horseradish peroxidase by γ-aminobutyric acid and application in detection of H_2O_2. Int J Biol Macromol 136:597–606

22. Dhawane M, Deshpande A, Jain R, Dandekar P (2019) Colorimetric point-of-care detection of cholesterol using chitosan nanofibers. Sens Actuators B Chem 281:72–79
23. Zhang Y, Liu S, Li Y, Deng D, Si X, Ding Y, He H, Luo L, Wang Z (2015) Electrospun graphene decorated $MnCo_2O_4$ composite nanofibers for glucose biosensing. Biosens Bioelectron 66:308–315
24. Samie HA, Arvand M (2019) RuO_2 nanowires on electrospun CeO_2-Au nanofibers/functionalized carbon nanotubes/graphite oxide nanocomposite modified screen-printed carbon electrode for simultaneous determination of serotonin, dopamine and ascorbic acid. J Alloy Compd 782:824–836
25. Kim H, Lee I, Kwon Y, Kim BC, Ha S, Lee J-H, Kim J (2011) Immobilization of glucose oxidase into polyaniline nanofiber matrix for biofuel cell applications. Biosens Bioelectron 26:3908–3913
26. Sabu C, Henna TK, Raphey VR, Nivitha KP, Pramod K (2019) Advanced biosensors for glucose and insulin. Biosens Bioelectron 141:111201
27. Wang ZG, Wan LS, Liu ZM, Huang XJ, Xu ZK (2009) Enzyme immobilization on electrospun polymer nanofibers: An overview. J Mol Catal B Enzym 56:189–195
28. Haghju S, Bari MR, Abad MAK (2018) Affecting parameters on fabrication of β-D-galactosidase immobilized chitosan/poly (vinyl alcohol) electrospun nanofibers. Carbohydr Polym 200:137–143
29. Colangelo LM, Baeumner AJ (2012) Recent progress in the design of nanofiber-based biosensing devices. Lab Chip 12:2612–2620
30. Zhu H, Du ML, Zhang M, Wang P, Bao SY, Fu YQ, Yao JM (2013) Facile and green fabrication of small, mono-disperse and size-controlled noble metal nanoparticles embedded in water-stable polyvinyl alcohol nanofibers: High sensitive, flexible and reliable materials for biosensors. Sens Actuators B Chem 185:608–619
31. Sapountzi E, Braiek M, Vocanson F, Chateaux JF, Renault NJ, Lagarde F (2017) Gold nanoparticles assembly on electrospun poly(vinyl alcohol)/poly(ethyleneimine) /glucose oxidase nanofibers for ultrasensitive electrochemical glucose biosensing. Sens Actuators B Chem 238:392–401
32. Temoçin Z, İnal M, Gökgöz M, Yiğitoğlu M (2018) Immobilization of horseradish peroxidase on electrospun poly(vinyl alcohol)–polyacrylamide blend nanofiber membrane and its use in the conversion of phenol. Polym Bull 75:1843–1865
33. Rafighi P, Tavahodi M, Haghighi B (2016) Fabrication of a third-generation glucose biosensor using graphene-polyethyleneimine-gold nanoparticles hybrid. Sens Actuators B Chem 232:454–461
34. Pundir CS, Lata S, Narwal V (2018) Biosensors for determination of D and L- amino acids: a review. Biosens Bioelectron 117:373–384
35. Metkar SK, Girigoswami K (2019) Diagnostic biosensors in medicine – a review. Biocatal Agric Biotechnol 17:271–283
36. Pundir CS, Malik M, Chaudhary R (2019) Quantification of pyruvate with special emphasis on biosensors: a review. Microchem J 146:1102–1112
37. Zamani FG, Moulahoum H, Ak M, Demirkol DO, Timur S (2019) Current trends in the development of conducting polymers-based biosensors. TrAC Trends Anal Chem 118:264–276
38. Conway GE, Lambertson RH, Schwarzmann MA, Pannell MJ, Kerins HW, Rubenstein KJ, Dattelbaum JD, Leopold MC (2016) Layer-by-layer design and optimization of xerogel-based amperometric first generation biosensors for uric acid. J Electroanal Chem 775:135–145
39. Kong L, Rohaizad N, Nasir MZM, Guan J, Pumera M (2019) Micromotor-assisted human serum glucose biosensing. Anal Chem 91:5660–5666
40. Das P, Das M, Chinnadayyala SR, Singha IM, Goswami P (2016) Recent advances on developing 3rd generation enzyme electrode for biosensor applications. Biosens Bioelectron 79:386–397
41. Pakapongpan S, Poo-arporn RP (2017) Self-assembly of glucose oxidase on reduced graphene oxide-magnetic nanoparticles nanocomposite-based direct electrochemistry for reagentless glucose biosensor. Mat Sci Eng C 76:398–405
42. Paul A, Vyas G, Paul P, Srivastava DN (2018) Gold-nanoparticle-encapsulated zif-8 for a mediator-free enzymatic glucose sensor by amperometry. ACS Appl Nano Mater 1:3600–3607
43. Temoçin Z (2013) Modification of glassy carbon electrode in basic medium by electrochemical treatment for simultaneous determination of dopamine, ascorbic acid and uric acid. Sens Actuators B Chem 176:796–802
44. Scognamiglio V (2013) Nanotechnology in glucose monitoring: Advances and challenges in the last 10 years. Biosens Bioelectron 47:12–25
45. Guan H, Gong D, Song Y, Han B, Zhang N (2019) Biosensor composed of integrated glucose oxidase with liposome microreactors/chitosan nanocomposite for amperometric glucose sensing. Colloids Surf A 574:260–267
46. Lai J, Yi Y, Zhu P, Shen J, Wu K, Zhang L, Liu J (2016) Polyaniline-based glucose biosensor: a review. J Electroanal Chem 782:138–153
47. Caro A, Humblot V, Méthivier C, Minier M, Barbes L, Li J, Salmain M, Pradier CM (2010) Bioengineering of stainless steel surface by covalent immobilization of enzymes. physical characterization and interfacial enzymatic activity. J Colloid Interface Sci 349:13–18
48. Rodrigues RC, Ortiz C, Murcia AB, Torres R, Lafuente RF (2013) Modifying enzyme activity and selectivity by immobilization. Chem Soc Rev 42:6290–6307
49. Vaidya BK, Kuwar SS, Golegaonkar SB, Nene SN (2012) Preparation of cross-linked enzyme aggregates of L-aminoacylase via co-aggregation with polyethyleneimine. J Mol Catal B Enzym 74:184–191
50. Iqbal J, Iqbal S, Müller CE (2013) Advances in immobilized enzyme microbioreactors in capillary electrophoresis. Analyst 138:3104–3116
51. Anusha JR, Raj CJ, Cho BB, Fleming AT, Yu KH, Kim BC (2015) Amperometric glucose biosensor based on glucose oxidase immobilized over chitosan nanoparticles from gladius of Uroteuthis duvauceli. Sens Actuators B 215:536–543
52. Campbell AS, Islam MF, Russell AJ (2017) Intramolecular electron transfer through poly-ferrocenyl glucose oxidase conjugates to carbon electrodes: 1. sensor sensitivity, selectivity and longevity. Electrochim Acta 248:578–584
53. Márquez A, Jorquera CJ, Domínguez C, Berbel XM (2017) Electrodepositable alginate membranes for enzymatic sensors: An amperometric glucose biosensor for whole blood analysis. Biosens Bioelectron 97:136–142
54. Xu J, Sheng Q, Shen Y, Zheng J (2017) Enhanced direct electron transfer of glucose oxidase based on gold nanoprism and its application in biosensing. Colloids Surf A 529:113–118
55. Zhao W, Zhang R, Xu S, Cai J, Zhu X, Zhu Y, Wei W, Liu X (2018) Molecularly imprinted polymeric nanoparticles decorated with AuNPs for highly sensitive and selective glucose detection. Biosens Bioelectron 100:497–503
56. Alim S, Kafi AKM, Rajan J, Yusoff MM (2019) Application of polymerized multiporous nanofiber of SnO_2 for designing a bienzyme glucose biosensor based on HRP/GOx. Int J Biol Macromol 123:1028–1034
57. Liu C, Sheng Y, Sun Y, Feng J, Wang S, Zhang J, Xu J, Jiang D (2015) A glucose oxidase-coupled DNAzyme sensor for glucose detection in tears and saliva. Biosens Bioelectron 70:455–461
58. Liu Y, Nan X, Shi W, Liu X, He Z, Sun Y, Ge D (2019) A glucose biosensor based on the immobilization of glucose oxidase and Au nanocomposites with polynorepinephrine. RSC Adv 9:16439–16446

59. Guo Q, Liu L, Wu T, Wang Q, Wang H, Liang J, Chen S (2018) Flexible and conductive titanium carbide–carbon nanofibers for high-performance glucose biosensing. Electrochim Acta 281:517–524
60. Xu S, Zhang Y, Zhu Y, Wu J, Li K, Lin G, Li X, Liu R (2019) Facile one-step fabrication of glucose oxidase loaded polymeric nanoparticles decorating MWCNTs for constructing glucose biosensing platform: Structure matters. Biosens Bioelectron 135:153–159
61. Zhang M, Zhou G, Feng Y, Xiong T, Hou H, Guo Q (2016) Flexible 3D nitrogen-doped carbon nanotubes nanostructure: A good matrix for enzyme immobilization and biosensing. Sens Actuators B 222:829–838
62. Kowalewska B, Jakubow K (2017) The impact of immobilization process on the electrochemical performance, bioactivity and conformation of glucose oxidase enzyme. Sens Actuators B 238:852–861
63. Baghayeri M, Veisi H, Motlagh MG (2017) Amperometric glucose biosensor based on immobilization of glucose oxidase on a magnetic glassy carbon electrode modified with a novel magnetic nanocomposite. Sens Actuators B 249:321–330
64. Zhang Y, Li X, Li D, Wei Q (2020) A laccase based biosensor on AuNPs-MoS_2 modified glassy carbon electrode for catechol detection. Colloids Surf B 186:110683